Supplementary materials:
Effect of tabs on the shear layer dynamics of a jet in crossflow

Nicholas Morse and Krishnan Mahesh†

Department of Aerospace Engineering and Mechanics, University of Minnesota, Minneapolis, MN 55455, USA

1. Supplementary movie descriptions

(i) Movie 1. Animation of an isocontour of instantaneous Q-criterion colored by $\omega_z D/\overline{U}_{\text{jet}}$ for the upstream tab at $R = 2$.

(ii) Movie 2. Animation of an isocontour of instantaneous Q-criterion colored by $\omega_z D/\overline{U}_{\text{jet}}$ for the upstream tab at $R = 4$.

(iii) Movie 3. Animation of an isocontour of instantaneous Q-criterion colored by $\omega_z D/\overline{U}_{\text{jet}}$ for the 45° tab at $R = 2$.

(iv) Movie 4. Animation of an isocontour of instantaneous Q-criterion colored by $\omega_z D/\overline{U}_{\text{jet}}$ for the 45° tab at $R = 4$.

2. Supplementary centerplane statistics

Figures with statistics on the centerplane are presented to permit closer comparison to the non-tabbed jet of Iyer & Mahesh (2016). Figure 1(*a*-*c*) shows contours of mean spanwise vorticity ($\overline{\omega}_z$) on the centerplane for the non-tabbed jet, upstream tab, and 45° tab, respectively, at $R = 2$. The upstream and downstream shear layers are clearly distinguished by the opposing signs of $\overline{\omega}_z$. Also shown in these plots are streamlines originating at the center, upstream side, and downstream side of the jet. The upstream and downstream streamlines align well with the contours of mean spanwise vorticity near the jet exit. The same is true for these streamlines in figure 2(*a*-*c*), which shows the same contours for $R = 4$. Figure 1(*d*-*f*) shows contours of mean pressure for each configuration at $R = 2$. As observed by Iyer & Mahesh (2016), a high pressure region resides in front of the jet due to the crossflow stagnation, next to which the upstream shear layer appears as a region of low pressure. Comparing the non-tabbed jet and the upstream tab, we find that this low pressure region is appears weaker and delayed for the upstream tab. The stagnation pressure below the tab is also visible, which produces a large adverse pressure gradient within the nozzle. For each configuration, the minimum of pressure occurs in the recirculation region behind the jet column, which is shown with a dashed contour line of $\overline{u} = 0$. This pressure minimum matches the description of Iyer & Mahesh (2016), although the downstream shear layer also exhibits low pressures. For $R = 4$,

† Email address for correspondence: kmahesh@umn.edu

the stagnation region in front of the jet is not as visible in contours of mean pressure (figure 2(d-f)) due to the lower relative magnitude of the crossflow velocity. The upstream tab delays the pressure drop in the USL compared to the non-tabbed jet, but a stronger global minimum in pressure occurs for this configuration after the upstream and downstream shear layers meet. For both the upstream tab and 45° tab at $R = 4$, there is a stronger low pressure region behind the jet column than for the non-tabbed jet.

Additionally, the mean $\overline{u}$ and $\overline{v}$ velocity components are shown in figures 1(g-i,j-l) and 2(g-i,j-l) for full comparison between the jet configurations. We note that for $R = 2$, the x-velocity along the USL streamline for the upstream tab in figure 1h is reduced compared to the non-tabbed jet for $x/D > 4$, while the opposite trend occurs for the 45° tab (figure 1i). Additionally, there are changes in the recirculation zones behind the jet, with greater differences observed in $\overline{u}$ than for $\overline{v}$, which appears more similar between the jet configurations.

REFERENCES

Iyer, P.S. & Mahesh, K. 2016 A numerical study of shear layer characteristics of low-speed transverse jets. *Journal of Fluid Mechanics* **790**, 275–307.

Regan, M.A. & Mahesh, K. 2019 Adjoint sensitivity and optimal perturbations of the low-speed jet in cross-flow. *Journal of Fluid Mechanics* **877**, 330–372.

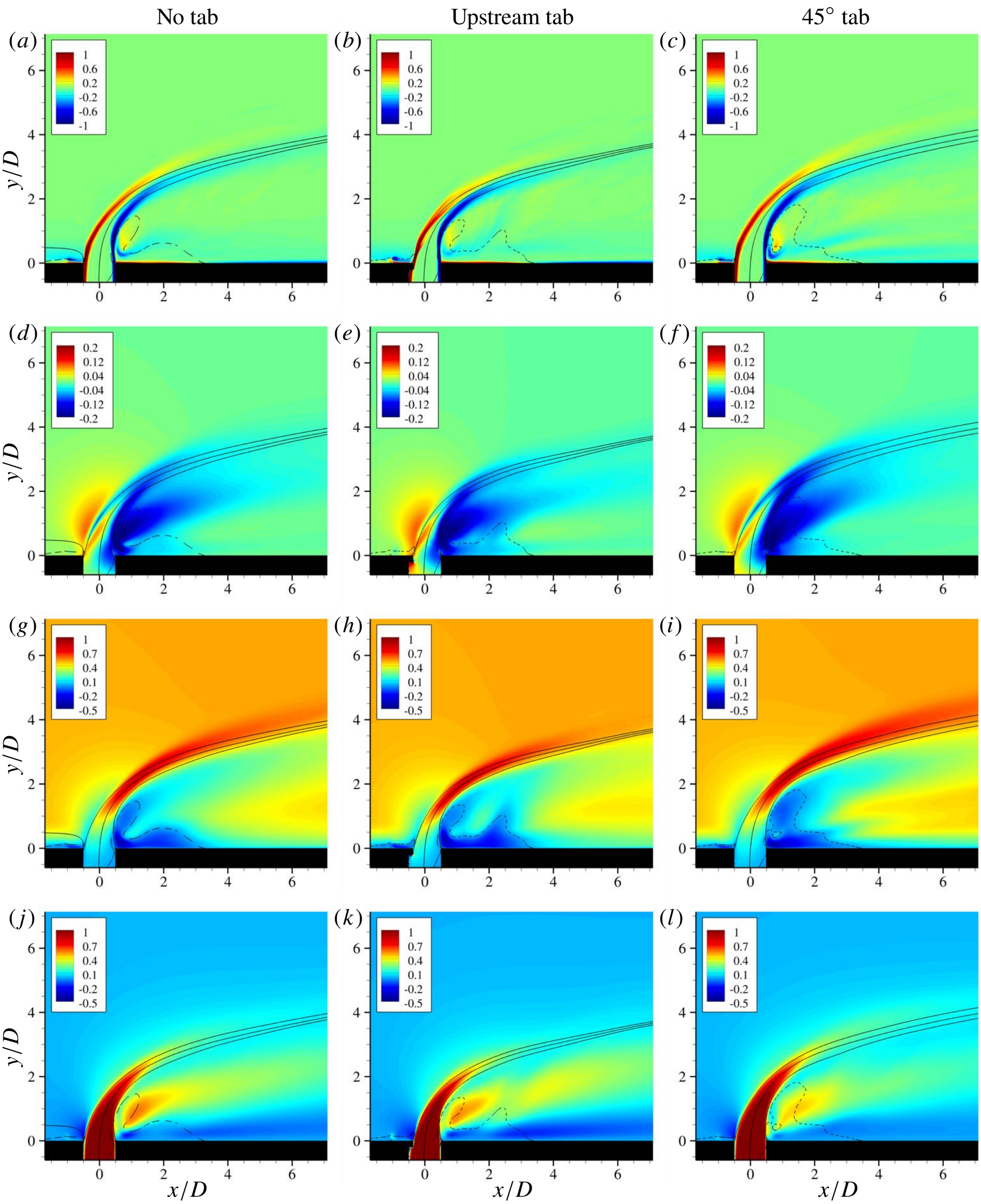

Figure 1: Contours of $\overline{\omega}_z D/\overline{U}_{\text{jet}}$ (*a*-*c*), $\overline{p}/\rho\overline{U}_{\text{jet}}$ (*d*-*f*), $\overline{u}/\overline{U}_{\text{jet}}$ (*g*-*i*), and $\overline{v}/\overline{U}_{\text{jet}}$ (*j*-*l*) on the centerplane for $R = 2$. Mean streamlines from the upstream edge, center, and downstream edge of the nozzle are shown as solid black lines and the contour line for $\overline{u} = 0$ (– – – –) is shown to mark recirculation zones. Results are shown for the non-tabbed jet from Regan & Mahesh (2019) (left column), the upstream tab (middle column), and the 45° tab (right column).

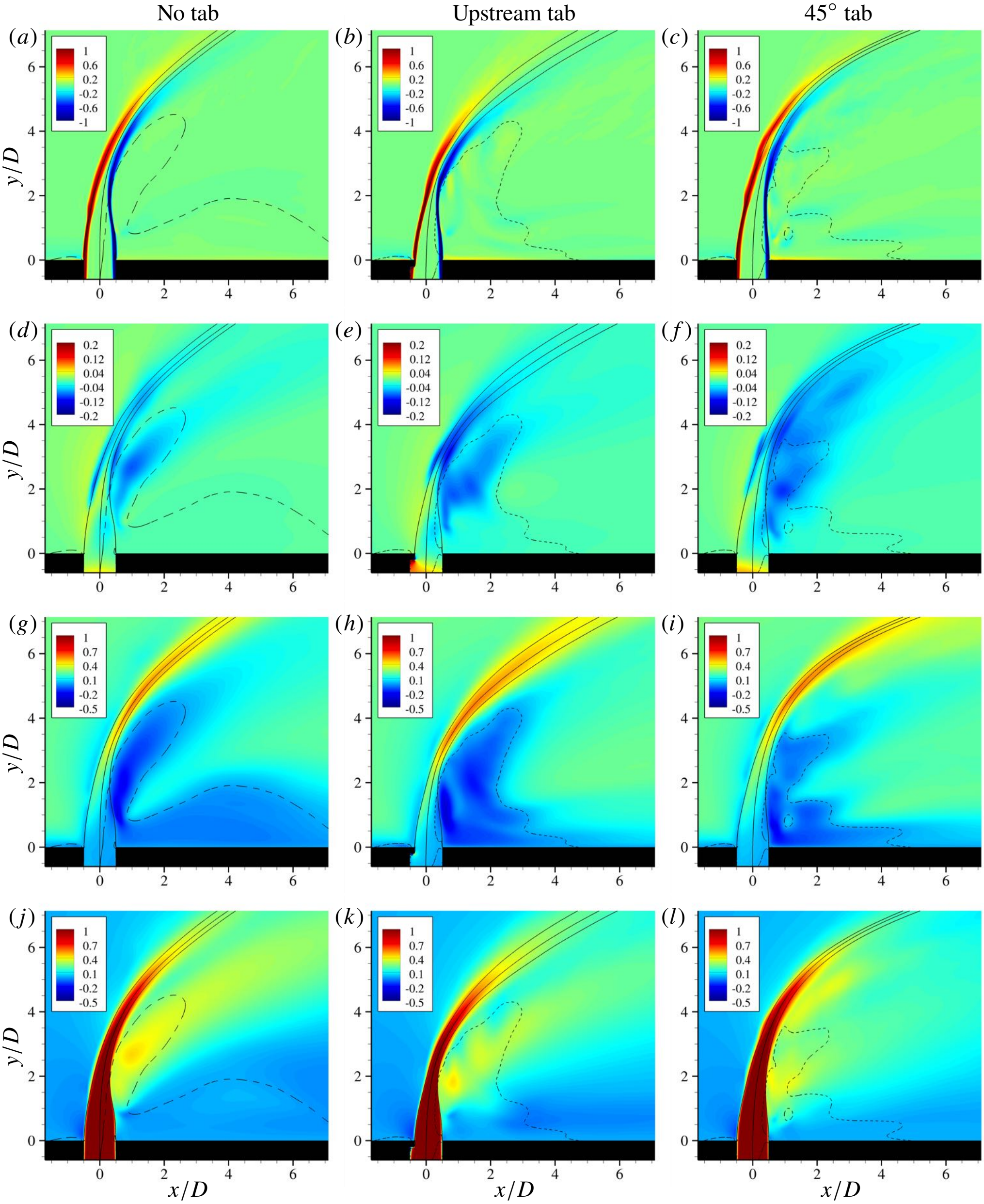

Figure 2: Contours of $\overline{\omega}_z D/\overline{U}_{\text{jet}}$ (*a-c*), $\overline{p}/\rho\overline{U}_{\text{jet}}$ (*d-f*), $\overline{u}/\overline{U}_{\text{jet}}$ (*g-i*), and $\overline{v}/\overline{U}_{\text{jet}}$ (*j-l*) on the centerplane for $R = 4$. Mean streamlines from the upstream edge, center, and downstream edge of the nozzle are shown as solid black lines and the contour line for $\overline{u} = 0$ (– – – –) is shown to mark recirculation zones. Results are shown for the non-tabbed jet from Regan & Mahesh (2019) (left column), the upstream tab (middle column), and the 45° tab (right column).